Observation of $PM_{2.5}$ using a combination of satellite remote sensing and low-cost sensor network in Siberian urban areas with limited reference monitoring

Changqing Lin,[1] Lev D. Labzovskii,[2,*] Hugo Wai Leung Mak,[3] Jimmy C.H. Fung,[1,4] Alexis K.H. Lau,[1,5] Samuel Takele Kenea,[2] Muhhamad Bilal,[6] Joshua D. Vande Hey,[7] Xingcheng Lu,[1] Jun Ma[5]

[1]Division of Environment and Sustainability, The Hong Kong University of Science and Technology, Hong Kong, China

[2]Climate Research Division, National Institute of Meteorological Sciences (NIMS), Seogwipo, Jeju-Do, 63568, Korea

[3]Faculty of Engineering, The Chinese University of Hong Kong, Hong Kong, China

[4]Department of Mathematics, Hong Kong University of Science and Technology, Hong Kong, China

[5]Department of Civil and Environmental Engineering, The Hong Kong University of Science and Technology, Hong Kong, China

[6]School of Marine Science, Nanjing University of Information Science and Technology, Nanjing 210044, China

[7]School of Physics and Astronomy, Earth Observation Science Group, University of Leicester, Leicester, United Kingdom

Corresponding Author:

* Address: Climate Research Division, National Institute of Meteorological Sciences (NIMS), Seogwipo, Jeju-Do, 63568, Republic of Korea. Email: labzowsky@gmail.com (Lev D. Labzovskii).

ABSTRACT: The lack of reference ground-based $PM_{2.5}$ observation leads to large gaps in air quality information, particularly in many areas of the developing world. This study investigated a new solution for urban air-quality monitoring in regions with limited reference ground-based monitoring. We developed an observation-based method by combining satellite remote-sensing techniques and a newly established low-cost sensor network to estimate long-term $PM_{2.5}$ concentrations over Krasnoyarsk, a highly industrialized Siberian city. First, a physical model was developed to estimate $PM_{2.5}$ concentrations using satellite remote-sensing with the aid of ground-based meteorological and radiosonde observations. Observations from the ground-based sensor network were then used to calibrate the deviations in the satellite-derived $PM_{2.5}$ concentrations. The results show that the satellite-based $PM_{2.5}$ concentrations obtained by our physical model were in good agreement with the sensor observations (R = 0.78 on the monthly scale). The deviation in satellite-derived annual $PM_{2.5}$ concentrations resulted from data restrictions that occurred at noon and data loss in winter were identified as 20% and 30%, respectively. The regional transport of smoke from forest wildfires increased $PM_{2.5}$ concentration to 150 $\mu g/m^3$ in the summer 2018. The average $PM_{2.5}$ concentrations in the urban districts could reach 35 $\mu g/m^3$, which far exceeded the World Health Organization air quality guideline. These results underscore the good ability of our new method to determine $PM_{2.5}$ concentrations in regions with limited reference ground-based monitoring. Use of sensor and meteorological observations greatly improved satellite detection of $PM_{2.5}$ concentration. In addition, our method has the potential for global application to improve determination of $PM_{2.5}$ concentrations, especially in sparsely monitored regions.

Keywords: Satellite; $PM_{2.5}$; Low-cost sensor; Siberia; Air quality

1. INTRODUCTION

Given the adverse effects of fine particulate matter ($PM_{2.5}$) on human health, $PM_{2.5}$ concentrations should be accurately monitored (Crouse et al., 2012; Guo et al., 2018). It is particularly important to monitor $PM_{2.5}$ concentrations in large urban areas, which contain millions of people in conditions of deteriorated air quality (Baklanov et al., 2016). $PM_{2.5}$ concentrations have traditionally been monitored by ground-based networks operated by government agencies (Rohde and Muller, 2015). However, such networks often fail to provide sufficient observational coverage for urban air quality monitoring. The resulting lack of governmental $PM_{2.5}$ data may have caused long-term deficiencies in air quality measurements in less-developed countries. Recent advances in satellite-based remote sensing and low-cost sensors are new opportunities to supplement incomplete conventional monitoring datasets from these regions (Pinder et al., 2019).

Using satellite-detected aerosol optical depth (AOD) to estimate $PM_{2.5}$ concentration is an effective tool to fill the data gaps in government-led ground-based observations (Chan et al., 2018; Lin et al., 2018). The estimation requires an understanding of the vertical distribution, hygroscopic growth, and characteristics of aerosols (Lin et al., 2016; Liu, 2014). A range of statistical models has been established to elucidate the link between AOD and $PM_{2.5}$ concentration using methods such as machine learning (Di et al., 2016; Xiao et al., 2018) and geographically and temporally weighted regression (Guo et al., 2017; He and Huang, 2018). These statistical models require sufficient ground-based $PM_{2.5}$ measurements as the training datasets, so their use is difficult in vast regions outside developed countries, where the ground-based monitoring coverage is sparse (Liu, 2014).

Satellite-based estimations of $PM_{2.5}$ concentrations in these poorly-monitored regions have to date relied on chemical transport models (CTMs) to simulate AOD-$PM_{2.5}$ relationships (van

Donkelaar et al., 2010). These CTM-based methods have no imposed restrictions on ground $PM_{2.5}$ measurements, but they impose heavy computational demands. Thus, each computation is subject to certain intrinsic uncertainties, such as those arise from aerosol vertical distribution and optical properties (van Donkelaar et al., 2006; Jin et al., 2019). It is therefore important to develop alternative observation-based AOD-$PM_{2.5}$ algorithms for estimation of $PM_{2.5}$ concentrations in these poorly monitored regions.

Technological progress has led to the development of miniaturized low-cost sensor devices with sufficient sensitivity for air quality monitoring (Kumar et al., 2015; Morawska et al., 2018). There has been considerable investigation of the utility of low-cost air-quality sensors, and there is a growing consensus that they could provide valuable information when used appropriately for suitable applications (WMO, 2018), such as providing indicative and supplementary data rather than regulatory data. These miniaturized sensors are less bulky, less expensive and easier to deploy and manage, than the reference instruments (Snyder et al., 2013).

Although $PM_{2.5}$ datasets with limited accuracy may be obtained from only a single sensor (Borrego et al., 2016; Castell et al., 2017), the integration of large numbers of sensors into a network can yield useful and realistic information about a city's air quality (Schneider et al., 2017). Some stationary sensor networks have already been established as pilot projects for air quality monitoring in complex environments, such as urban areas (Gao et al., 2015; Semple et al., 2015) and airports (Popoola et al., 2018). The United States Environmental Protection Agency (U.S. EPA) has confirmed the necessity of extending the existing urban air-quality monitoring systems by introducing low-cost sensors (U.S. EPA, 2014). Long-term measurements from low-cost sensor networks may ultimately be used to complement the mapping of urban air-quality and to assist in the calibration and evaluation of deviations in satellite-derived $PM_{2.5}$ concentration data.

When urban air quality measurements are severely lacking, the efforts of non-governmental urban air-quality monitoring can encourage citizen action by informing broad audiences about a city's air quality. Such a situation has already developed in Krasnoyarsk, a large industrial center of Siberia. Krasnoyarsk is susceptible to air quality deterioration due to numerous urban emission sources from chemical and metallurgical industries (including one of the world's largest aluminum smelting plants), coal-burning power plants, and transportation (Khleboporos et al., 2012). Moreover, the region around Krasnoyarsk frequently experiences summer wildfires (Conard and Davidenko, 1996), which leads to a reduction in ground visibility and cause long-term episodes of air pollution in the city (Damoah et al., 2004). Public concern about air quality has evolved rapidly in recent years. This concern coincides with an increase in the number of people with pulmonary disease (Artyukhov et al., 2015). A 2018 report from the Ministry of Environmental Management concluded that air pollution in Krasnoyarsk was "very high," and the city was included in the list of the most polluted urban areas in Russia (Ministry of Environmental Management, 2018).

To provide more local, accessible data, an unofficial $PM_{2.5}$ monitoring network named "Nebo" ("sky" in Russian) was founded in Krasnoyarsk. The numerous low-cost sensors in this network have rapidly covered the city's entire urban area; measurements have been collected since 2017, and the data have been periodically released for public access. Moreover, the Nebo network regularly reports unhealthy or very unhealthy air quality conditions, based on the widely-recognized EPA indices. The Nebo network has developed a high level of trust with a wide range of users in Krasnoyarsk (>25,000 people follow its activities) and is currently making recommendations related to outdoor activities for a broad audience within the city. This citizen-science action is positive, but further scientific investigation of the information potential of the network is needed, which motivated this study.

This study used Krasnoyarsk as a case study for alternative solutions in urban air-quality monitoring in regions with poor reference monitoring. We used satellite remote-sensing and newly developed ground-based low-cost sensors (the Nebo sensor network) as primary tools to measure the $PM_{2.5}$ concentrations in Krasnoyarsk. Within the main scope of the study, we analyzed the agreement of low-cost sensors with available reference observations to determine the validity of the sensor measurements. Then, by applying an observation-based method to estimate the distribution of $PM_{2.5}$ concentration, we characterized $PM_{2.5}$ variation in Krasnoyarsk during a 2-year period (2017 to 2018), including the anomalous pollution events. Finally, we evaluated the method's performance, uncertainty, and long-term applicability.

2. DATA AND METHODS

2.1 Study region

Figure 1 shows the topography of the study region around Krasnoyarsk (92.55°E to 93.15°E, 55.7°N to 56.3°N). Krasnoyarsk is on the Yenisei river in Siberia, Russia, and is surrounded by forested mountains to the south and west and by plains to the north and east. It is the regional center of Krasnoyarsk Krai, which is part of the so-called "donor" region of Russia that supplies 50% of the country's gross domestic product (GDP). Krasnoyarsk's economy is highly industrialized, and some industrial facilities around it are unprecedented and have global importance. For instance, ~3% of the world's aluminum is produced there. This industrialized economy has invariably created environmental challenges in Krasnoyarsk and its surroundings, such as degraded air quality. Moreover, Krasnoyarsk's mountainous landscape and its location in the basin of the Yenisei River make the city more susceptible to fog and haze formation. The frequent cold temperatures generate temperature inversion layers, whereby a layer of mountain-derived cold air traps polluted air from the industrial sources in the atmosphere over Krasnoyarsk (Gosteva et al., 2019).

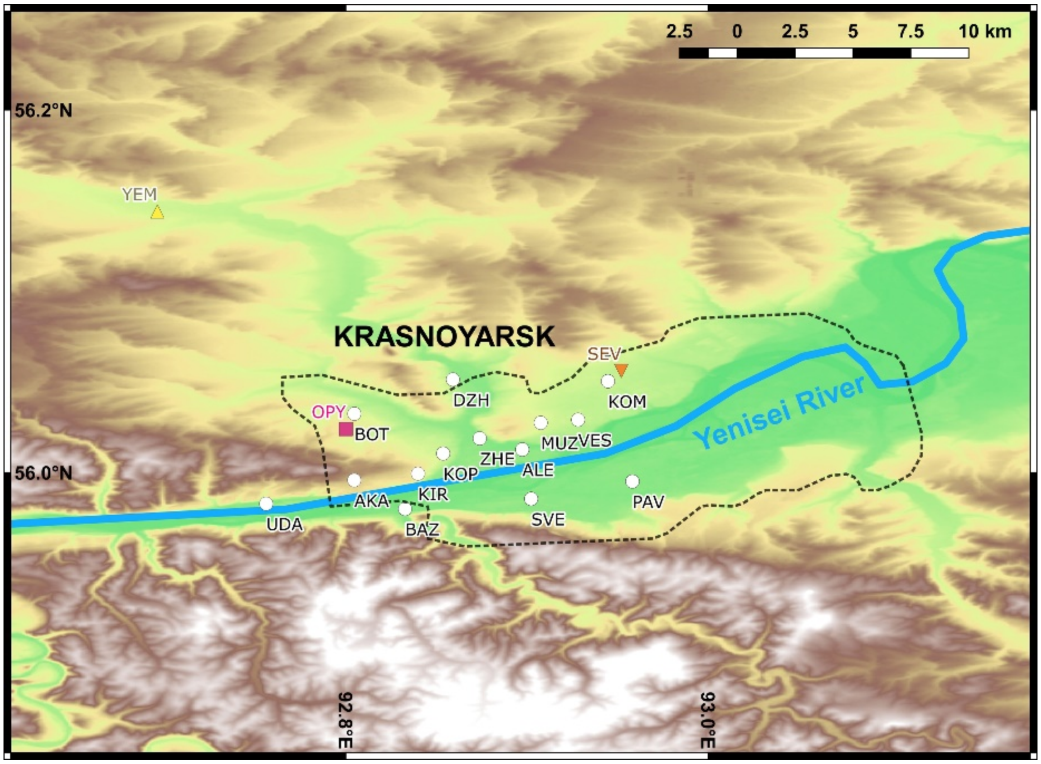

Figure 1. Topography of the study region around Krasnoyarsk. White points represent measurements within the ground-based $PM_{2.5}$ sensor network, red square represents the ground meteorological station for visibility and relative humidity measurements, yellow triangle represents the radiosonde station, and orange triangle represents the $PM_{2.5}$ reference monitoring station.

2.2 Ground-based observations of $PM_{2.5}$ in Krasnoyarsk

2.2.1 Reference observation of $PM_{2.5}$

$PM_{2.5}$ concentration was measured using the β-attenuation monitor (BAM) at Severniy (SEV, 56.07°N and 92.94°E) station in February 2018. Its location is shown by the orange triangle in Figure 1. This reference data was provided by the Ministry of Environment to Nebo network as a validation dataset for the newly introduced sensors. The BAM analyzer is manufactured by MetOne Instruments. According to the governmental procurement activities, more BAM analyzers are expected to be installed within Krasnoyarsk in the near future (http://zakupki.gov.ru/223/purchase/public/download/download.html?id=45643315).

2.2.2 Sensor observation of $PM_{2.5}$

The establishment of the Nebo network continues in Krasnoyarsk. The network uses identical units of the AirVisual Node to measure $PM_{2.5}$ concentration. The operation of the AirVisual Node is based on the common light-scattering principle (Singer and Delp, 2018). The AirVisual machine-learning algorithms then calibrate and validate the sensor using temperature and humidity values. AirVisual staff conducted a field evaluation of the sensor's performance in Beijing in June 2015 (Ng, 2016), and the comparison between observations from AirVisual sensors and the reference BAM instrument on a daily basis during this period shown good agreement (R = 0.91). Independent laboratory evaluation of AirVisual sensors using DustTrak has also confirmed that these units reliably and realistically quantify $PM_{2.5}$ (Tan, 2017), and all sensors were delivered to the network installation team after the laboratory calibration was conducted by the manufacturer.

$PM_{2.5}$ concentration was recorded at each measurement site at a high frequency of 20 minutes and then averaged to obtain hourly estimates. The Nebo network has introduced 14 stations for $PM_{2.5}$ monitoring, as indicated by white points in Figure 1 (see detailed information in Table S1). This study used the observations from 11 stations (which by January 2019 had accumulated data for more than 6 months) to calibrate and evaluate satellite observation. The sensor observations at Komsomolskiy (KOM) station, which is 900 m from SEV station, were used from February 2018 to determine the sensor's performance. All sensors were mounted outside in special boxes situated on the second floors of residential buildings of a similar type. This setup was used to ensure as much as possible that the sensors were free from exposure to very strong emission sources and could thus measure $PM_{2.5}$ with good spatial representativeness. The data were uploaded by the AirVisual global project to an air pollution app that offers free access to a large air quality database that includes observations from thousands of AirVisual Nodes distributed around the world (https://www.airvisual.com).

2.3 Radiosonde observations

A key parameter in all existing AOD-$PM_{2.5}$ models is the planetary boundary layer height (PBLH), which determines the extent to which vertical mixing occurs (He and Huang, 2018; Ma et al., 2016). Common methods for deriving PBLH have used vertical profiles of meteorological quantities (Guo et al., 2016; Johnson et al., 2001). In this context, radiosondes remain the standard for upper-level air monitoring and provide the most accurate information of vertical profiles of the meteorological variables (Cimini et al., 2013). Radiosondes are thus often adopted as a data source for operational determination of PBLH (Seibert et al., 2000).

We acquired the radiosonde data from Yemelyanovo (YEM, 56.18°N and 92.62°E) station in Krasnoyarsk from the World Meteorological Organization's global telecommunications system, as shown by the yellow triangle in Figure 1. Radiosondes are routinely launched twice a day at 7:00 am and 7:00 pm local time. We adopted the method proposed by Holzworth (1964, 1967) to produce diurnal variation in the PBLH at an interval of 1 hour. The Holzworth method has been widely used in a range of meteorological and environmental studies (Karimian et al., 2016; Yang et al., 2013). It assumes a constant potential temperature within the PBL. The PBLH is identified as the height at which the upper potential temperature equal to ground potential temperature. Based on the estimated hourly PBLH data, the daily noontime average of PBLH (from 11:00 am to 2:00 pm) was obtained to match the time of satellite observation.

2.4 Meteorological observation

Hourly surface meteorological parameters, such as relative humidity (RH) and visibility (L), at Opytnoe Pole (OPY, 56.03°N and 92.75°E, red square in Figure 1) were also acquired from the World Meteorological Organization. The atmosphere was moderately moist in Krasnoyarsk, and the average noontime RH was 61.2% ± 16.5% within this 2-year period. The visibility ranged from 0 to 10 km, with all values above 10 km recorded as 10 km; such visibility upper limits are frequently registered not only in Siberia but also in regions such as America, Africa, the Middle East, and southern Asia (i.e., an upper limit can be 10 km or 16 km in these places). The surface aerosol extinction coefficient ($\sigma_{a,0}$) can be quantified from visibility by $\sigma_{a,0} = 3.912/L$ (Koschmieder, 1925).

2.5 Satellite observation of $PM_{2.5}$

2.5.1 Satellite observation of AOD

The Moderate Resolution Imaging Spectroradiometer (MODIS) instruments aboard Terra and Aqua measure AOD (Chu et al., 2002). In this study, MODIS C6 level-2 AOD data in Krasnoyarsk for 2017 and 2018 were acquired. The AOD data were retrieved using the dark-target algorithm over land (Levy et al., 2013). Based on the nominal resolution of the MODIS AOD, we created 400 grid cells at a spatial resolution of 0.03° × 0.03° that covered the study region. The measurements from two satellites were averaged to represent the daily noontime value. MODIS AOD data are often missing due to the presence of clouds and high surface reflectance (Liu, 2014). Figure S1 shows the sample size of the satellite-based daily AOD within the study region for different months from 2017 to 2018. The samples were counted when satellite observations were available in at least 25% of the area within the study region. It was found that the satellite observations were poor in winter, mainly because snow and ice surfaces in these high-latitude regions generate high surface reflectance (van Donkelaar et al., 2006). The data loss in winter should be therefore considered when we estimate annual $PM_{2.5}$ concentrations via satellite.

2.5.2 Satellite-based estimation of $PM_{2.5}$

We adopt and extend an observational data-driven algorithm to retrieve $PM_{2.5}$ concentrations, showing in supplementary material (Lin et al., 2015). The algorithm introduces aerosol scale height (H), integrated humidity coefficient (γ'), and integrated reference value under dry-air conditions (K).

The scale height H can be estimated from the ratio of the satellite-based AOD and the visibility-derived $\sigma_{a,0}$. Similar to most other regions, the visibility dataset was affected by an upper limit of 10 km in Krasnoyarsk. The PBLH provided additional information to characterize the aerosol vertical distribution. The scale height can be larger than PBLH when a significant concentration of aerosols accumulates above the PBL. We therefore introduce a ratio (A) of scale height to the PBLH. Spatial distribution of the $PM_{2.5}$ concentration can be estimated as follow:

$$PM_{2.5} = \frac{\frac{AOD}{A \cdot PBLH}}{K \cdot \left(\frac{1-RH}{1-RH_0}\right)^{-\gamma'}} \tag{1}$$

The PBLH and RH derived from the radiosonde and meteorological stations represent atmospheric conditions over the entire Krasnoyarsk area. The γ' and K values are prerequisite parameters in our $PM_{2.5}$ estimation model, and both are associated with aerosol characteristics (Lin et al., 2019). The average γ' and K values across China, where aerosols covered various categories, were estimated to be 0.50 ± 0.32 and 5.14 ± 1.56 m^2/g, respectively (Lin et al., 2015). In the monitoring-limited regions, assumptions of both γ' and K values are required. In this work, we began the estimate of $PM_{2.5}$ concentration in Krasnoyarsk based on the average γ' and K values derived from the Chinese study. Because actual γ' and K values over Krasnoyarsk were likely to differ from the values over China, we discuss the effect of the difference in aerosol characteristics between China and Krasnoyarsk in Section 3.3 and assess the possible uncertainties based on these assumptions in Section 3.5.

2.6 HYSPLIT backward trajectory model

We exploited the Hybrid Single-Particle Lagrangian Integrated Trajectory (HYSPLIT) model to track the origin of air masses in Krasnoyarsk. The HYSPLIT model is one of the most common models for conducting back-trajectory analysis and is based on source-receptor relationships (Rolph et al., 2017). In this study, the computation of the backward trajectory used the meteorological fields of the Global Data Assimilation System with a spatial resolution of 0.5° × 0.5°. The model ran in a backward trajectory regime for 12 hours, starting from 12:00 UTC in Krasnoyarsk (56.01°N, 92.87°E) at 200 m above sea level. The backward trajectories of air parcels were calculated using a free-access online platform developed by the Air Resources Laboratory of National Oceanic and Atmospheric Administration (https://ready.arl.noaa.gov/HYSPLIT.php).

3. RESULTS

3.1 Evaluation of ground-based sensor observations

To evaluate the performance of the Nebo network sensors, we compared $PM_{2.5}$ concentration observations from one sensor with the reference $PM_{2.5}$ measurement. The BAM observations from SEV station in February 2018 had been provided to the Nebo network by governmental agencies. Figure S2 compares the time series of hourly $PM_{2.5}$ concentrations from the sensor at KOM station with the reference BAM monitor at SEV station. Good agreement was obtained between the $PM_{2.5}$ concentrations from the sensor and BAM observation. Both of sensor and BAM monitoring detected those high $PM_{2.5}$ pollution episodes.

Figure 2 shows regression relationship between hourly $PM_{2.5}$ concentrations from the sensor and reference BAM monitoring. Slope and intercept were estimated to be 0.95 and 0.41

μg/m³, respectively. Good agreement between the sensor and reference monitoring was obtained with a correlation coefficient (R) of 0.94 (N = 672) and a mean absolute percentage deviation within 20%. The monthly average $PM_{2.5}$ concentration from the sensor and BAM were estimated to be 55.4 μg/m³ and 57.7 μg/m³, respectively. The systematic deviation in the monthly average $PM_{2.5}$ concentration was -2.3 μg/m³, which was insignificant and was within 5%. Such high agreement also outperformed the experiment conducted by the AirVisual group in Beijing. Moreover, this node-to-BAM agreement was as high as that of the previous dataset from the Chinese city of Xian (R = 0.93–0.95) (Gao et al., 2015) and higher than that of the dataset from the U.S. city of Oakland (R = 0.80–0.84) (Holstius et al., 2014).

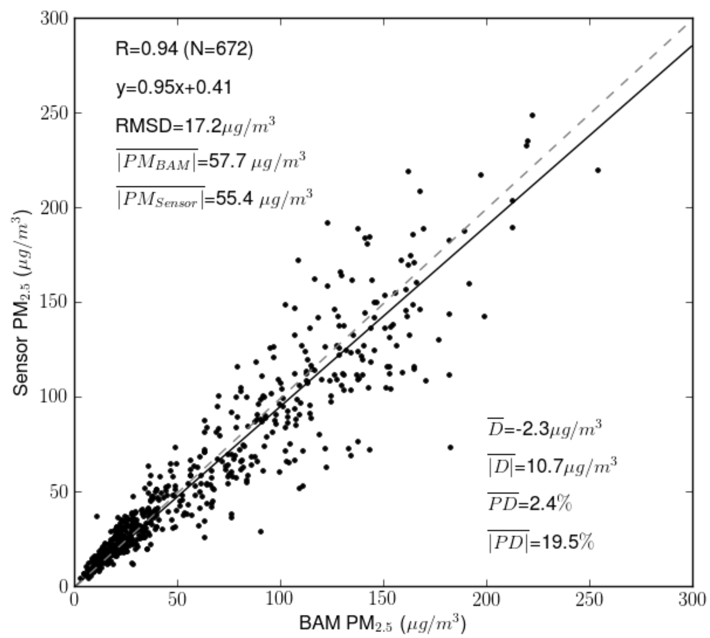

Figure 2. Regression relationship between hourly $PM_{2.5}$ concentrations from the sensor at KOM station and the reference BAM monitoring data from SEV station in February 2018. The statistical metrics include correlation coefficient (R), root-mean-square deviation (RMSD), mean deviation ($\overline{D}$), mean absolute deviation ($\overline{|D|}$), mean percentage deviation ($\overline{PD}$), and mean absolute percentage deviation ($\overline{|PD|}$).

To evaluate the performance of each sensor, we further compare temporal variation in the hourly $PM_{2.5}$ concentrations at different stations. Figure 3 shows the correlation coefficient between hourly $PM_{2.5}$ concentrations for each pair of stations during the second half year of 2018 (i.e., from July to December), when observations were available at all stations. Average sample size was 3697. The correlation coefficient ranged from 0.45 to 0.89 with an average of 0.72. The lowest correlation coefficients were associated with $PM_{2.5}$ concentration at AKA station, which was on the westernmost side of the city. The larger distances between AKA station and other stations could lead to these lower correlation coefficients. Temporal variation in $PM_{2.5}$ concentrations at AKA and its neighboring stations (e.g., BAZ and KIR stations), however, was highly consistent with a correlation coefficient exceeded 0.8. These results suggest the good performance of all sensors from the network.

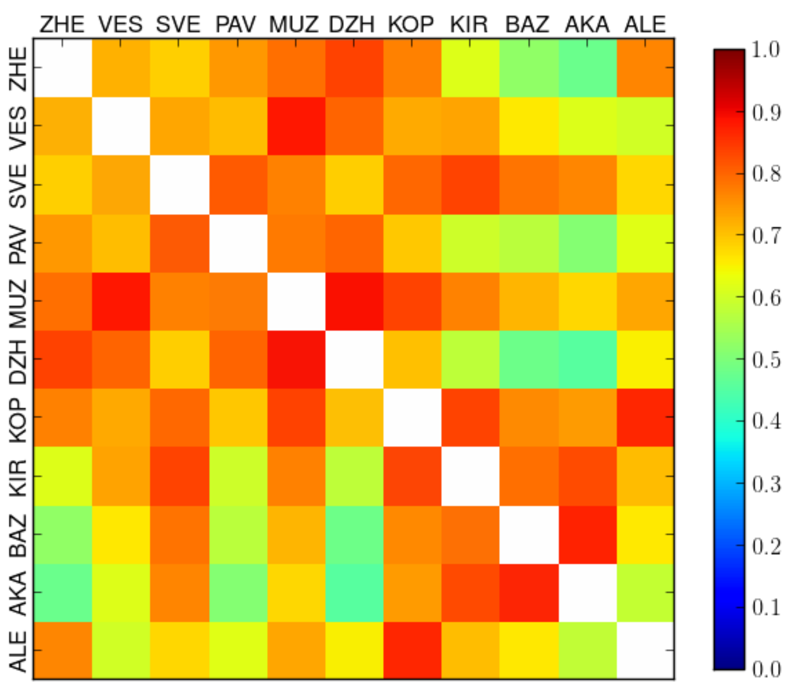

Figure 3. Correlation coefficient between hourly $PM_{2.5}$ concentrations for each pair of stations during the second half year of 2018 (i.e., from July to December).

Validation of all sensors of the Nebo network throughout all seasons of the year would have been an enormous undertaking given the limited data access and the gaps in the spatial coverage of the government monitoring. Nevertheless, within the observed conditions, the high sensor-to-BAM agreement and insignificant systematic bias suggest good field performance of the $PM_{2.5}$ sensors in Krasnoyarsk, which implies that the use of sensors after laboratory calibration was acceptable to achieve the desired goals of our study. In case of detecting a significant sensor's bias after laboratory calibration, we would recommend an adjustment of the sensor data using the regression equations.

3.2 Retrieving PBLH and scale height

To define the vertical mixing within our method of $PM_{2.5}$ data retrieval, we plotted the time series of the noontime average PBLH (from 11:00 am to 2:00 pm) at the radiosonde station from 2017 to 2018 (see the black line in Figure S3). In general, the noontime PBLHs in spring and summer were higher than those in autumn and winter. Such seasonal patterns were similar to those observed in radiosonde or lidar datasets from northern China (Chu et al., 2019; Guo et al., 2016); these studies have shown that high near-surface wind speed and intense solar radiation favors the development of the boundary layer in spring and summer. The scale height H was estimated from the ratio of the satellite-based AOD and the visibility-derived $\sigma_{a,0}$. The red triangles show the noontime scale height at the meteorological station on specific dates, when satellite observations were available and the ground visibility was within the upper limit (i.e., 10 km).

Figure S4 shows the seasonal average ratio (A) of the scale height to PBLH in Krasnoyarsk during the study period. The seasonal average ratios for spring (MAM), summer (JJA), and autumn (SON) were estimated to be 0.99 ± 0.52, 1.70 ± 0.62, and 0.99 ± 0.37, respectively. The high ratio in summer suggests that approximately 40% of aerosols appeared above the PBL, which resulted from the vertical convection and regional transport of aerosols such as wildfire smoke.

3.3 Comparison between satellite-based and ground-based $PM_{2.5}$ concentrations

We applied the method described in Section 2.5.2 to estimate $PM_{2.5}$ concentrations using satellite remote-sensing data, coupled with radiosonde and ground meteorological observations. The satellite-based estimation of $PM_{2.5}$ concentration used average values of γ' and K obtained from China (i.e., 0.50 and 5.14 m^2/g) (Lin et al., 2015). We compared the agreement in $PM_{2.5}$ concentrations between satellite and Nebo sensor observations. Thus, Figure 4 shows correlation coefficients between the satellite-derived and ground-based daily noontime $PM_{2.5}$ concentrations during the study period. The correlation coefficients ranged from 0.36 at PAV station to 0.87 at AKA station (mean, 0.57 ± 0.14). These correlation coefficients were comparable to those from the eastern United States (R = 0.30 – 0.80) and higher than those from the western United States (R < 0.30) obtained with the CTM-based model (van Donkelaar et al., 2006). Our results suggest that the observation-based model predicted the temporal variations in $PM_{2.5}$ concentration as accurately as the simulation-based model.

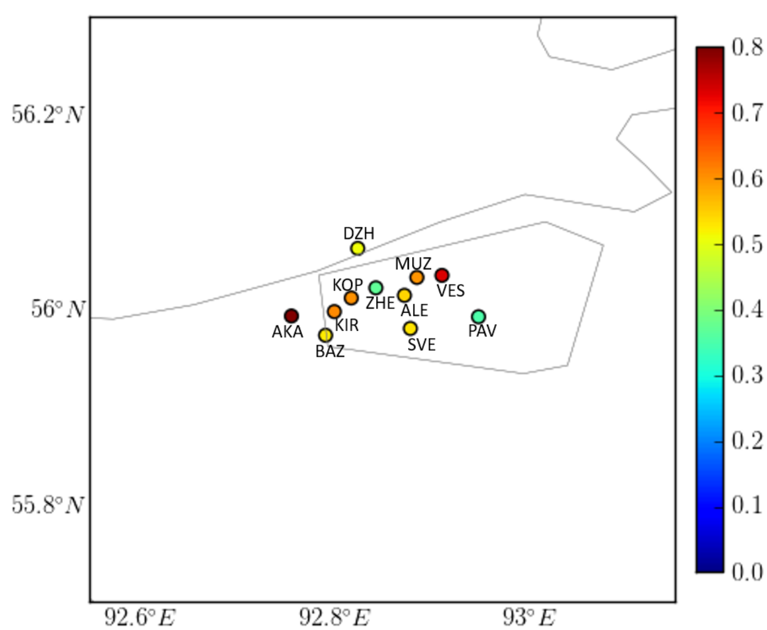

Figure 4. Correlation coefficient between satellite-derived and ground-observed daily noontime $PM_{2.5}$ concentrations from various sensors during the study period.

However, systematic deviations were observed between the satellite-derived and sensor-observed $PM_{2.5}$ concentrations, in that the 2-year averages of the satellite-derived $PM_{2.5}$ concentrations were consistently higher than the corresponding sensor observations. On average, these satellite-derived $PM_{2.5}$ concentrations were overestimated by 5.92 $\mu g/m^3$ (i.e., 27.6% of sensor observations), which could have been due to the various chemical compositions and optical properties of aerosols over Krasnoyarsk compared to the aerosols over China. That is, Siberian wildfires mean that Krasnoyarsk experiences a higher average loading of carbonaceous aerosols (e.g., elemental and organic carbons) than does China (Smolyakov et al., 2014). The K value in Krasnoyarsk is thus expected to be higher than that in China because of the strong light extinction efficiency of the carbonaceous aerosols (Watson, 2002). Therefore, we made an assumption and used a higher K value of 6.56 m^2/g for the Krasnoyarsk data, 27.6% higher than the average value in China. This eliminated the systematic error within the satellite-derived data but did not affect the correlation coefficient between the satellite-derived and sensor-observed daily $PM_{2.5}$ concentrations.

Figure 5 compares of the satellite-derived and ground-observed daily noontime $PM_{2.5}$ concentrations from the sensor at SVE station, which has the longest data record (i.e., measurements started in June 2017). In the Figure, the blue points on both panels show the time series of the ground-observed daily noontime $PM_{2.5}$ concentration from 2017 to 2018, and the red points show the time series of the satellite-derived daily noontime AOD and $PM_{2.5}$ concentrations, respectively. Notably, after the conversion from AOD to $PM_{2.5}$ concentration, the correlation coefficient increased from 0.51 to 0.54 (N = 78) during the study period. In particular, the correlation coefficient substantially increased from 0.09 to 0.67 (N = 24) in 2017.

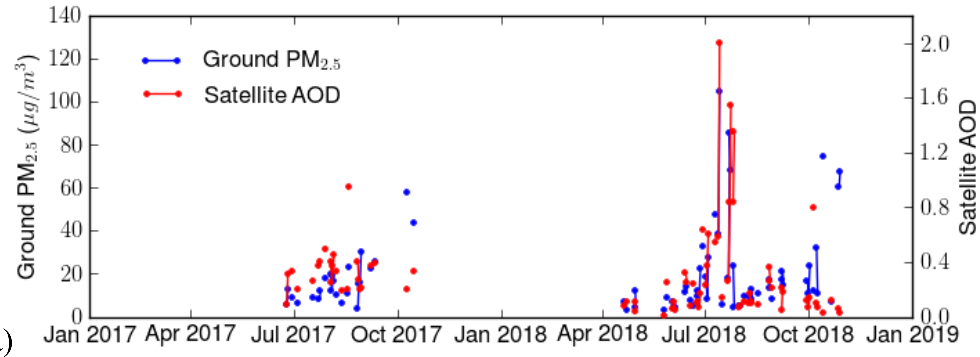

(a)

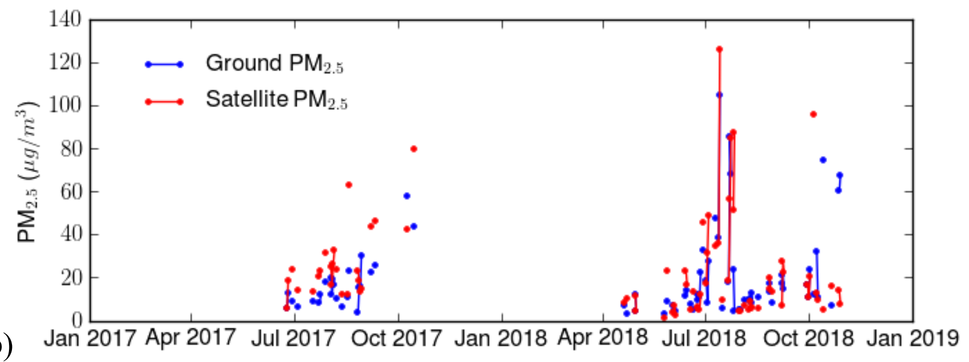

(b)

Figure 5. Comparison of satellite-derived and ground-observed daily noontime $PM_{2.5}$ concentrations from the sensor at SVE station from 2017 to 2018. Blue points in (a) and (b) show the time series of the ground-observed daily noontime $PM_{2.5}$ concentrations. Red points in (a) and (b) show the time series of the satellite-derived daily noontime AOD and $PM_{2.5}$ concentrations, respectively.

3.4 Characterization of $PM_{2.5}$ concentration variation

We combined Nebo monitoring observations and spaceborne data to characterize $PM_{2.5}$ concentration variations in Krasnoyarsk in the years for which observations were available (2017 and 2018) and during the anomalous pollution events.

3.4.1 Spatiotemporal variation of $PM_{2.5}$ concentration

At first, we analyzed the temporal variability of $PM_{2.5}$ concentration during 2017 and 2018. Figure S5 shows the time series of $PM_{2.5}$ concentrations from 11 sensors within this period. The $PM_{2.5}$ concentrations varied considerably. The highest $PM_{2.5}$ concentrations (>200 μg/m^3) were frequently observed in winter (e.g., January and February) and in July 2018. The high $PM_{2.5}$ concentrations in winter were seemingly driven by enhanced emissions from heating systems and by weather conditions that were unfavorable for pollution dispersion (Mikhailuta et al., 2009).

Figure S6 demonstrates the diurnal variation in $PM_{2.5}$ concentration from the sensor observations. These variations were characterized based on the averaged $PM_{2.5}$ concentrations obtained from the four sensors at SVE, PAV, LOP, and ALE stations with full data coverage in 2018. The results show that the $PM_{2.5}$ concentration reached its peak at 2:00 pm. We also plot the corresponding $PM_{2.5}$ concentrations at noontime (indicated by the red solid line), for when satellite observations were available. We discovered that the noontime average $PM_{2.5}$ concentration was higher than the 24-h average by 5.24 μg/m^3 (i.e., 20.0% of the 24-h average).

Because satellite observations were only available at approximately noon, a correction factor was needed to represent the degree of diurnal $PM_{2.5}$ variation to obtain robust long-term averages. To obtain the monthly average $PM_{2.5}$ concentration, we therefore applied a correction factor of 1.20 to the satellite-derived monthly average of noontime $PM_{2.5}$ concentrations. This correction factor was essential because the use of satellite-derived $PM_{2.5}$ concentrations mainly focused on the use of long-term averages (e.g., monthly and annual averages).

We further evaluated the correlation between satellite-derived monthly average $PM_{2.5}$ concentrations against ground-based observations from all sensors during 2017 and 2018 period (shown in Figure 6). A good correlation coefficient of 0.78 (N = 74) was obtained. This city-scale correlation is comparable to national-scale comparisons seen in other studies (van Donkelaar et al., 2010, 2015; Geng et al., 2015; Peng et al., 2016). The root-mean-square deviation, mean deviation, and mean percentage deviation were estimated to be 7.1 μg/m^3, 1.4 μg/m^3, and 18.1%, respectively. We once again emphasize that the application of the constant correction factor does not affect the correlation coefficient between the satellite-derived and sensor-observed monthly $PM_{2.5}$ concentrations.

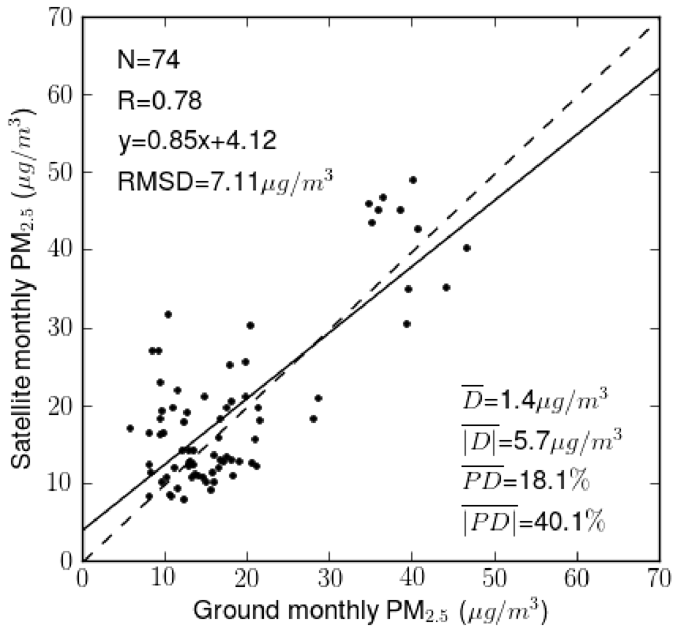

Figure 6. Evaluation of satellite-derived monthly averaged $PM_{2.5}$ concentration against ground-based observations from all sensors in Krasnoyarsk during 2017 and 2018. Statistical metrics include correlation coefficient (R), root-mean-square deviation (RMSD), mean deviation ($\overline{\mathrm{D}}$), mean absolute deviation ($\overline{|\mathrm{D}|}$), mean percentage deviation ($\overline{\mathrm{PD}}$), and mean absolute percentage deviation ($\overline{|\mathrm{PD}|}$).

The solid line in Figure S7 shows the monthly variation of the average $PM_{2.5}$ concentrations from the four sensors at SVE, PAV, LOP, and ALE stations with a full data coverage in 2018. It revealed the distinct pollution features in Krasnoyarsk. The highest monthly $PM_{2.5}$ concentration was observed in winter (as high as 63 μg/m^3 in February). Another peak of $PM_{2.5}$ concentration was observed in summer (40 μg/m^3 in July). Both peaks are also displayed in Figure S5, which depicts results derived from measurements at 11 stations. Because the satellite observations were only available from April to October (the 7 months shown by the red line), another correction factor that represented the degree of monthly $PM_{2.5}$ variation was needed to obtain the annual average.

We found that the annual average $PM_{2.5}$ concentration was higher than the 7-month average by 7.86 μg/m^3 (i.e., 30.0% of the annual average), which indicates that the use of uncorrected satellite data leads to severe underestimation of the annual $PM_{2.5}$ concentrations in high-latitude regions such as Krasnoyarsk. To obtain a more accurate annual average of $PM_{2.5}$ concentration, we therefore divided the satellite-derived 7-month average of $PM_{2.5}$ concentration by 0.7.

After the correction factors were determined, we identified the spatial distribution of the $PM_{2.5}$ concentrations in Krasnoyarsk by plotting the satellite-derived averages from 2017, 2018, and 2017–2018 (shown in left, middle, and right panels of Figure 7, respectively). The points in the middle panel represent the annual average $PM_{2.5}$ concentrations from the four sensors with full data coverage in 2018. The mean deviation of the annual averaged $PM_{2.5}$ concentrations from satellite and sensor observations was 1.4 μg/m^3 (i.e., 5.3% of sensor observation). Satellite observations show that the highest $PM_{2.5}$ concentrations were present over the geographical center and the southern coast of the city in 2017 and 2018 period. In this area, the $PM_{2.5}$ concentrations ranged from 29.5 μg/m^3 (Central district) to 35.0 μg/m^3 (Sverdlovskiy District) in 2017. In 2018, the same area had $PM_{2.5}$ concentrations ranging from 24.7 μg/m^3 (Central district) to 33.9 μg/m^3 (Sverdlovskiy District). Therefore, the 2-year average $PM_{2.5}$ concentrations in the central and southern districts of Krasnoyarsk could reach 35 μg/m^3, which far exceeds the World Health Organization (WHO) Air Quality Guideline (AQG) for annual $PM_{2.5}$ standards (i.e., 10 μg/m^3).

The higher $PM_{2.5}$ concentration in the geographical center of the city and southern districts underscores the high pollutant emission and unfavorable dispersion conditions in this area, and the increased negative effects on health that these conditions would have. In total, the spatial average of the 2-year $PM_{2.5}$ concentration over 400 grid cells within the study region was estimated to be 23.1 ± 3.5 μg/m^3. This estimate was ~63% higher than the national averaged $PM_{2.5}$ concentration (14.2 μg/m^3) in Russia in 2013 (Brauer et al., 2016).

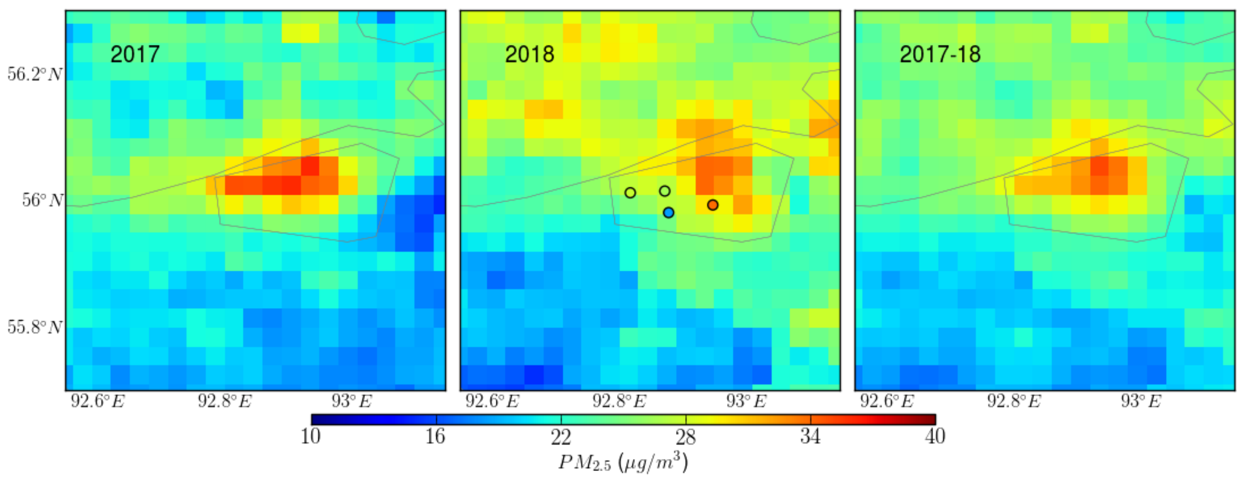

Figure 7. Left and middle panels show spatial distribution of satellite-derived annual averaged $PM_{2.5}$ concentrations in 2017 and 2018, and right panel shows corresponding 2-year average distribution. Points in middle panel represent annual average $PM_{2.5}$ concentrations from the four sensors with full data coverage in 2018.

3.4.2 $PM_{2.5}$ pollution episode in July 2018

As aforementioned, $PM_{2.5}$ concentration had a distinct spike in July 2018. Panel a of Figure 8 shows the time series of $PM_{2.5}$ concentrations at PAV station in the middle of July 2018, where it can be seen that $PM_{2.5}$ concentrations reached 150 μg/m^3 on July 13. We make use of the true-color images acquired from the MODIS instrument aboard Aqua satellite (shown in panel b) for further investigation. In the figure, the red points represent the areas of active fire hotspots. We found that on July 13, 2018, the large forest areas in the close vicinity of Krasnoyarsk were engulfed by the wildfires. Analysis of MODIS images reveals that the massive smoke plumes originated from wildfires in the northeastern direction from Krasnoyarsk. Krasnoyarsk was directly exposed to the increased aerosol loading driven by smoke particles. Additional analyses of HYSPLIT back trajectory (shown in panel c) have also supported the smoke-transport hypothesis, that is, that the air masses transported smoke particles directly from the hotspot regions to Krasnoyarsk.

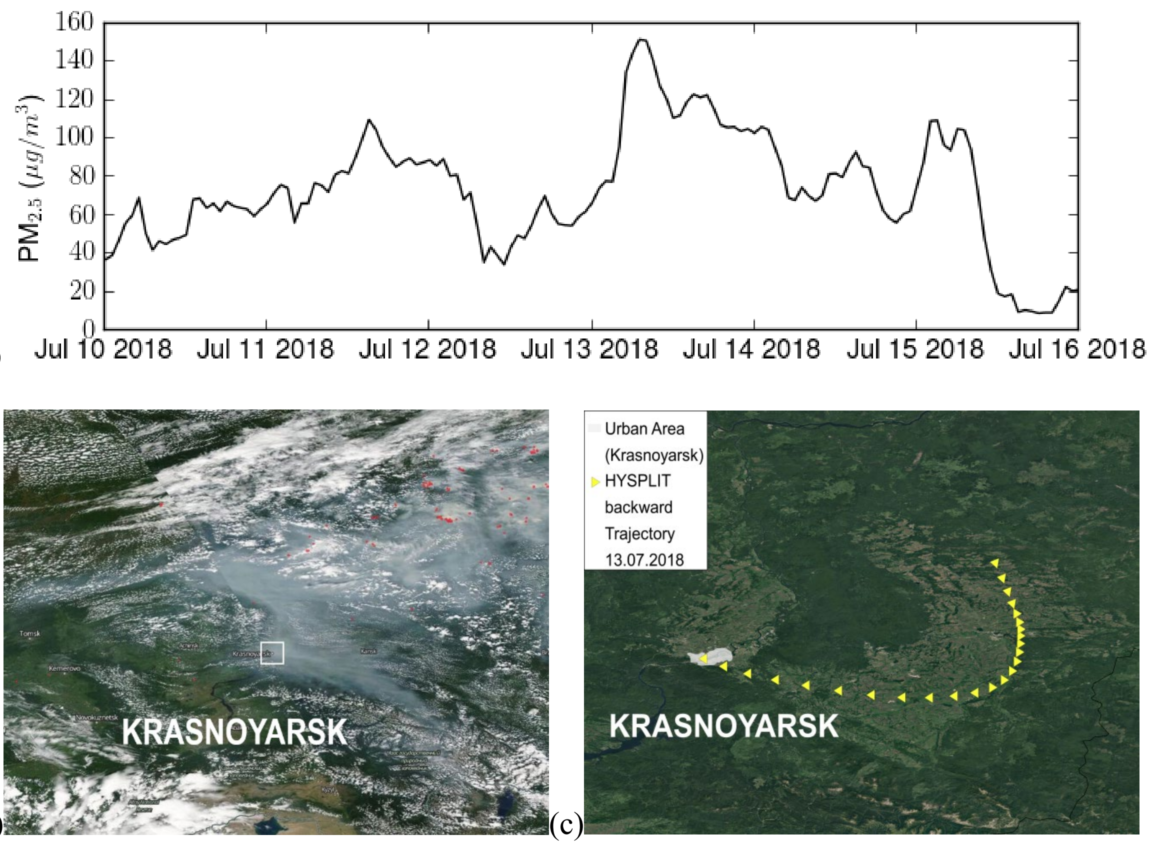

(a) (b) (c)

Figure 8. (a) Time series of $PM_{2.5}$ concentration at PAV station in the middle of July 2018. (b) True-color images acquired from the MODIS instrument aboard Aqua satellite on July 13, 2018. Red points identify actively burning wildfires. (c) HYSPLIT back-trajectory analysis using 12-h setting (yellow triangles) near Krasnoyarsk (white pixels).

3.5 Performance and uncertainties of the observation-based method

In this section, we evaluate the performance and describe the uncertainties of our proposed method and data sources used in this study.

3.5.1 Evaluation of our method compared to other methods

The statistical AOD-$PM_{2.5}$ methods used extensive $PM_{2.5}$ observational data to train the models and therefore tended to have lower estimation errors (He and Huang, 2018; Liu, 2014; Ma et al., 2016). Their requirement for extensive ground observations hinders their application in the regions with large observational data gaps (like most developing countries) or with restricted access to $PM_{2.5}$ data (e.g., most ex-Soviet countries including Russia). In such regions, traditional AOD-$PM_{2.5}$ methods have to rely on simulation results from the CTMs (e.g., GEOS-Chem model) to give an estimate of $PM_{2.5}$ concentrations.

Figure S8 shows the spatial distribution of the satellite-derived annual $PM_{2.5}$ concentrations based on a CTM-based model in the study region for 2016 (downloaded from http://fizz.phys.dal.ca/~atmos/martin/?page_id=140). The spatial pattern of $PM_{2.5}$ concentrations was similar to the results obtained in this study. In particular, the $PM_{2.5}$ concentrations were elevated within the urban area of Krasnoyarsk and in the close vicinity of the city. The spatial average of $PM_{2.5}$ concentrations obtained from the CTM-based model was approximately 16.0 $\mu g/m^3$, which was 30% lower than the concentrations obtained in this study. Such a deviation could stem from the uncertainties of model simulation and satellite data loss. This would potentially cause bias in exposure and health impact assessments using this data. Future studies should further compare data sets obtained from different sources.

3.5.2 Uncertainties of the satellite-derived $PM_{2.5}$ concentrations

Major uncertainty in the $PM_{2.5}$ concentrations estimated from satellite data stems from the input factors such as satellite-based AOD, PBLH, the ratio (A) of scale height to PBLH, and the γ'

and K values. Using the same PBLH algorithm as in Krasnoyarsk, we also produced the PBLH from radiosonde data in Hong Kong, for which ground-based lidar observations are available. Evaluation of the radiosonde-derived daily noontime PBLH using the lidar observations showed good agreement, with a correlation coefficient of 0.63 (N = 2075) and a percentage deviation of around 20% (Su et al., 2017).

It is also essential to consider the difference between the scale height and PBLH for regions like Krasnoyarsk, in which a large proportion of aerosols are transported above the PBL. Without introduction of the ratio of scale height to PBLH, the $PM_{2.5}$ estimation can be greatly biased during summer. In this study, we used the seasonal average of such a ratio because the AOD-visibility pairs were limited during the investigation period. If more visibility data are available, more information on the scale height and its association with PBLH can be obtained.

The γ' and K are prerequisite parameters in our $PM_{2.5}$ estimation model. Both are associated with aerosol characteristics. The use of the average K value from China (i.e., 5.14 ± 1.56 m^2/g) resulted in uncertainty in the $PM_{2.5}$ concentration of about 30%. Given the higher loading of carbonaceous aerosols, we used a higher K value to reduce the deviation in the satellite-derived $PM_{2.5}$ concentration for Krasnoyarsk.

To assess the uncertainty caused by using the average γ' value from China (i.e., 0.50 ± 0.32), we performed Monte Carlo simulation, in which we set the values of AOD, PBLH, A, RH, and K as 0.25, 1 km, 1, 61%, and 6.56 m^2/g, respectively. We generated 10,000 γ' values from a normalized distribution with a mean and standard deviation of 0.50 and 0.32, respectively. We then estimated $PM_{2.5}$ concentrations using these γ' values. The frequency distribution of the estimated $PM_{2.5}$ concentration is shown in Figure S9. The estimated mean (and standard deviation) $PM_{2.5}$ concentration was 31.0 ± 4.3 μg/m^3, which suggests that the uncertainty caused by direct use of the γ' value from China was less than 15%. Future studies can refine the γ' and K values when more detailed information on local aerosol characteristics are available.

3.5.3 Uncertainties of sensor observations

We performed several quality control processes to avert the failure of sensors. First, once the cheap nodes for $PM_{2.5}$ observations are calibrated in laboratory conditions, they will endure for ~2 years in the stable conditions without instrumental-related deviations. Our work deals with 1-2 years observations. Second, an automated algorithm sets observation value to N.A. once observation is physically failed. Third, we performed statistical-based “flagging” the observation data beforehand. We determined that not more than 4% of point observations were found in the statistically unrealistic interval for each station. Statistical anomaly is defined as range outside +/- 3 times of standard deviation from hourly mean. Such observations were removed beforehand. Most malignant observations were found in BOT station (3.9%). However, it is not a problem in the data since BOT station had provided prominently less observations in total than other stations. The agreement between low number of total observations at BOT and the presence of the statistical anomalies indirectly approves the validity of automated sensor algorithm (i.e., sensor adequately and frequently switches off at station with issues). At every other station, the percentages of the anomalies found per each station are: 2.9% at SVE, 1.9% at UDA, 3.3% at VES, 3.1% at AKA, 3.2% at DZH, 3.1% at MUZ, 2.9% at BAZ, 3.4% at KIR, 2.4% at KOP, 2.3% at ADY, 3.5% at KOM, 3.6% at ZHE, 3.5% at PAV, 3.9% at BOT.

Collocation of BAM-to-node experiment is peculiarly difficult in Krasnoyarsk because of three malignant factors. Foremost, the access to air quality observations is severely limited and there is a lack of comprehensive study that can approve that existing governmental sensors are accurate enough. As we know, the first study about evaluating air quality observations from governmental network is under the process. We underline that their effort is independent from our study and do not provide any synergistic retrieval for $PM_{2.5}$ monitoring. Once they open all these datasets or manage to publish their study, it will be easier to compare their observations with our method. At second, any actions with BAM instrument on-site is challenging for the team behind this paper. BAM collocation was initiated by Russian government as a result of exceptional top-down decision. After that, we had not noticed any will to make additional experiment from the governmental side. Despite we want as much as possible inter-comparison data, the combined manpower-funding limitation for the on-site work does not allow to obtain any additional BAM sensors in a commercial way. At third, it is a common knowledge about peculiarly difficult situation with air quality observations in the post-USSR countries. The current situation description is easily found in the modern research literatures (Strukova et al., 2019). All in all, although one BAM is not adequate for very comprehensive study, but in our situation and as a first step towards better understanding of air quality status in industrial city, it is a good start. These factors are actually the reasons why our work is so helpful in the hindered situation with poor air quality monitoring, constrained access to most of data, and lack of adequate funding.

Based on the previously discussed results of the Beijing AirVisual comparison and the AirVisual-BAM comparison in Krasnoyarsk, the credibility of the Nebo sensor network for measuring $PM_{2.5}$ concentration was deemed satisfactory. The uncertainty in the validity of data from low-cost sensors stems from factors such as meteorological influence, unpredictable drift or unknown seasonality in measurement bias, sensor saturation, and degradation of the sensors, along with potential variation in sensitivity to aerosols of various properties.

During the month-long comparison, the Nebo sensor exhibited good agreement with the BAM reference instruments (R = 0.94). Field calibration of each sensor from the Nebo network was a major challenge due to the limited reference observations. To address these challenges, we used only the aggregated and averaged information from sensor observations at multiple stations (e.g., averaged diurnal and monthly variations in $PM_{2.5}$ concentration from the four sensors at SVE, PAV, LOP, and ALE stations) to calibrate the satellite observations. Our evaluation of the monthly average $PM_{2.5}$ concentrations in February 2018 from the sensor using reference monitoring suggested an insignificant systematic bias (<5%).

4. DISCUSSION

This work aimed to find alternative solutions for urban air-quality monitoring for regions with poor reference monitoring, based on a study conducted in Krasnoyarsk. Low-cost sensors and satellite observations were used to develop an observation-based method to estimate long-term $PM_{2.5}$ concentrations within the city for 2017–2018. Different approaches have unique advantages and can compensate for the weaknesses when they are deployed together (Pinder et al., 2019). Deployment of a few reference monitoring pairing with the low-cost sensors ensures the data quality and quantifies the uncertainty. The low-cost sensor network and satellite remote sensing then extend spatiotemporal coverage. The satellite-derived $PM_{2.5}$ concentrations showed good agreement with the sensor $PM_{2.5}$ concentrations ($R = 0.78$ on the monthly scale). The sensor $PM_{2.5}$ concentrations were used to correct the deviation in the satellite-derived annual $PM_{2.5}$ concentrations by 20%, resulting from data restriction at noontime, and by 30%, resulting from the data loss in winter. The deviation between the satellite-derived and sensor-observed annual $PM_{2.5}$ concentrations was <10%. Taken together, these data show that our method has satisfactory performance and reasonable uncertainties.

Our results have both local and global implications. From a local perspective, our results demonstrate that low-cost sensor data and synergy method are sufficiently accurate that they can be used to assist governmental urban air-quality monitoring. Given the high level of agreement between the BAM and the AirVisual Node with which it was compared, local policymakers may find it beneficial to co-locate multiple AirVisual sensors with their reference stations for an extended period of time. This will enable evaluation of the efficacy of these sensors as a potential supplemental source of information to aid understanding of sources and dispersion of pollution and of the effectiveness of interventions.

In particular, the method are applicable in cities like Krasnoyarsk, where significant emission sources are well known but insufficient quantitative information exists. Its use could pave the way for nationwide projects for air quality improvement. This aspect is particularly important for Russia because its Clean Air program consists of ambitious plans for improving urban air quality in 12 industrial cities (including Krasnoyarsk) by 2021 (Government of Russian Federation, 2019).

From a global perspective, our $PM_{2.5}$ estimation model relies on widely-available data and can thus be used to investigate $PM_{2.5}$ pollution trends and effects in poorly observed regions. Such investigations may help to reveal previously unreported effects of aerosols on the environment, health, and climate on global scales. The approach of Shaddick et al. (2018), which filled data gaps and assigned uncertainties, can be used to identify areas with predicted high exposures and high uncertainties, which can then be targeted by the new monitoring infrastructure. Understanding how the linkage of low-cost sensor networks and other observations can improve global estimates of $PM_{2.5}$ exposure is thus critical to realize the potential benefits of emerging lower-cost technologies. Therefore, the method developed here can be extended for global $PM_{2.5}$ monitoring applications in the foreseeable future, especially for poorly observed regions such as that in this study.

5. CONCLUSIONS

The lack of reference ground-based $PM_{2.5}$ observation has resulted in major gaps in air-quality information globally, particularly in many parts of the developing world. This study developed and validated an alternative solution for urban air-quality monitoring in regions such as Krasnoyarsk, which has limited reference ground-based monitoring. We developed an observation-based method by combining satellite remote-sensing techniques and a low-cost sensor network to estimate long-term $PM_{2.5}$ concentrations.

Our method met satisfactory requirements for providing high spatiotemporal $PM_{2.5}$ distributions for urban air quality monitoring. Our method has been applied for robust quantification of the $PM_{2.5}$ concentration in Krasnoyarsk for 2017 and 2018, resolving long-term ambiguity about aerosol distribution within the city. The $PM_{2.5}$ concentration in Krasnoyarsk during these years was 23.1 $\mu g/m^3$, which is 63% higher than the average $PM_{2.5}$ in Russia (14.2 $\mu g/m^3$). Seasonal variability in the $PM_{2.5}$ concentration over Krasnoyarsk in 2018 revealed two distinct peaks in winter (e.g., February) and summer (e.g., July). The peak in winter is likely to be due to increased heating and unfavorable pollution-dispersion conditions. During the pollution event in summer, the $PM_{2.5}$ concentrations reached 150 $\mu g/m^3$ as a result of smoke transport from forest wildfires.

Further studies should include three key steps. First, AirVisual sensors should be deployed alongside $PM_{2.5}$ reference monitors at a variety of urban and rural background locations to understand the sensors' response to various aerosol mixes. Second, further study is required to assess the spatial extent and resolution of the low-cost sensor sampling points and the site requirements of the sampling locations to provide the most accurate picture of $PM_{2.5}$ across a city or region using this technique. Finally, evaluation of how this nonregulatory but potentially quite accurate data can inform government and citizen stakeholders is needed to improve public health and policy.

Acknowledgments

This work was supported by the Science and Technology Plan Project of Guangdong Province of China (Grant No. 2017A050506003), the Research Grants Council of Hong Kong Government (Project No. T24/504/17), NSFC/RGC (Grant No. N_HKUST638/19), and the Fok Ying Tung Graduate School (NRC06/07.SC01). J. Vande Hey's contribution was funded by the Natural Environment Research Council of the UK (NE/N005406/1). Part of this work was supported by the Korean Meteorological Administration Research and the Development Program "Development and Assessment of IPCC AR6 Climate Change Scenario (1365003000)". We gratefully acknowledge Igor Schpekht and the entire team of Nebo monitoring for providing free access to the data from their sensors and for their strong support of our study. We also thank Oleg Yakubailik for providing relevant information about state-of-the-art conditions of urban air quality in Krasnoyarsk and the surrounding regions. The authors declare that they have no actual or potential competing financial interests.

Reference

Artyukhov, I.P., Arshukova, I.L., Dobretsova, E.A., Dugina, T.A., Shulmin, A.V., and Demko, I.V. (2015). Epidemiology of chronic obstructive pulmonary disease: a population-based study in Krasnoyarsk region, Russia. Int. J. Chron. Obstruct. Pulmon. Dis. *10*, 1781–1786.

Baklanov, A., Molina, L.T., and Gauss, M. (2016). Megacities, air quality and climate. Atmos. Environ. *126*, 235–249.

Borrego, C., Costa, A.M., Ginja, J., Amorim, M., Coutinho, M., Karatzas, K., Sioumis, Th., Katsifarakis, N., Konstantinidis, K., De Vito, S., et al. (2016). Assessment of air quality microsensors versus reference methods: The EuNetAir joint exercise. Atmos. Environ. *147*, 246–263.

Brauer, M., Freedman, G., Frostad, J., van Donkelaar, A., Martin, R.V., Dentener, F., Dingenen, R. van, Estep, K., Amini, H., Apte, J.S., et al. (2016). Ambient Air Pollution Exposure Estimation for the Global Burden of Disease 2013. Environ. Sci. Technol. *50*, 79–88.

Castell, N., Dauge, F.R., Schneider, P., Vogt, M., Lerner, U., Fishbain, B., Broday, D., and Bartonova, A. (2017). Can commercial low-cost sensor platforms contribute to air quality monitoring and exposure estimates? Environ. Int. *99*, 293–302.

Chan, T.-C., Zhang, Z., Lin, B.-C., Lin, C., Deng, H.-B., Chuang, Y.C., Chan, J.W.M., Jiang, W.K., Tam, T., Chang, L., et al. (2018). Long-Term Exposure to Ambient Fine Particulate Matter and Chronic Kidney Disease: A Cohort Study. Environ. Health Perspect. *126*, 107002.

Chu, D.A., Kaufman, Y.J., Ichoku, C., Remer, L.A., Tanré, D., and Holben, B.N. (2002). Validation of MODIS aerosol optical depth retrieval over land. Geophys. Res. Lett. *29*, MOD2-1-MOD2-4.

Chu, Y., Li, J., Li, C., Tan, W., Su, T., and Li, J. (2019). Seasonal and diurnal variability of planetary boundary layer height in Beijing: Intercomparison between MPL and WRF results. Atmospheric Res.

Cimini, D., De Angelis, F., Dupont, J.-C., Pal, S., and Haeffelin, M. (2013). Mixing layer height retrievals by multichannel microwave radiometer observations. Atmospheric Meas. Tech. *6*, 2941–2951.

Conard, S.G., and Davidenko, E.P. (1996). Fire in Siberian Boreal Forests — Implications for Global Climate and Air Quality. Int. Symp. Air Pollut. Clim. Change Eff. For. Ecosyst. *General Technical Report PSW-GTR-166*, 87–94.

Crouse, D.L., Peters, P.A., van Donkelaar, A., Goldberg, M.S., Villeneuve, P.J., Brion, O., Khan, S., Atari, D.O., Jerrett, M., Pope, C.A., et al. (2012). Risk of nonaccidental and cardiovascular mortality in relation to long-term exposure to low concentrations of fine particulate matter: a Canadian national-level cohort study. Environ. Health Perspect. *120*, 708–714.

Damoah, R., Spichtinger, N., Forster, C., James, P., Mattis, I., Wandinger, U., Beirle, S., Wagner, T., and Stohl, A. (2004). Around the world in 17 days - hemispheric-scale transport of forest fire smoke from Russia in May 2003. Atmospheric Chem. Phys. *4*, 1311–1321.

Di, Q., Kloog, I., Koutrakis, P., Lyapustin, A., Wang, Y., and Schwartz, J. (2016). Assessing PM2.5 Exposures with High Spatiotemporal Resolution across the Continental United States. Environ. Sci. Technol. *50*, 4712–4721.

van Donkelaar, A., Martin, R.V., and Park, R.J. (2006). Estimating ground-level PM2.5 using aerosol optical depth determined from satellite remote sensing. J. Geophys. Res. Atmospheres *111*.

van Donkelaar, A., Martin, R.V., Brauer, M., Kahn, R., Levy, R., Verduzco, C., and Villeneuve, P.J. (2010). Global estimates of ambient fine particulate matter concentrations from satellite-based aerosol optical depth: development and application. Environ. Health Perspect. *118*, 847–855.

van Donkelaar, A., Martin, R.V., Brauer, M., and Boys, B.L. (2015). Use of satellite observations for long-term exposure assessment of global concentrations of fine particulate matter. Environ. Health Perspect. *123*, 135–143.

Gao, M., Cao, J., and Seto, E. (2015). A distributed network of low-cost continuous reading sensors to measure spatiotemporal variations of PM2.5 in Xi'an, China. Environ. Pollut. *199*, 56–65.

Geng, G., Zhang, Q., Martin, R.V., van Donkelaar, A., Huo, H., Che, H., Lin, J., and He, K. (2015). Estimating long-term PM2.5 concentrations in China using satellite-based aerosol optical depth and a chemical transport model. Remote Sens. Environ. *166*, 262–270.

Gosteva, A.A., Matuzko, A.K., and Yakubailik, O.E. (2019). Detection of changes in urban environment based on infrared satellite data. IOP Conf. Ser. Mater. Sci. Eng. *537*, 062051.

Government of Russian Federation (2019). Federal Policy "About conducting experiment for regulating pollutants from emissions and about complementing the federal laws on decreasing atmospheric pollution." N 4483p-P9 (N 4483п-П9). Signed by D. Medvedev on 23.05.2019 in Moscow (document in Russian).

Guo, C., Zhang, Z., Lau, A.K.H., Lin, C.Q., Chuang, Y.C., Chan, J., Jiang, W.K., Tam, T., Yeoh, E.-K., Chan, T.-C., et al. (2018). Effect of long-term exposure to fine particulate matter on lung function decline and risk of chronic obstructive pulmonary disease in Taiwan: a longitudinal, cohort study. Lancet Planet. Health *2*, e114–e125.

Guo, J., Miao, Y., Zhang, Y., Liu, H., Li, Z., Zhang, W., He, J., Lou, M., Yan, Y., Bian, L., et al. (2016). The climatology of planetary boundary layer height in China derived from radiosonde and reanalysis data. Atmospheric Chem. Phys. *16*, 13309–13319.

Guo, Y., Tang, Q., Gong, D.-Y., and Zhang, Z. (2017). Estimating ground-level PM2.5 concentrations in Beijing using a satellite-based geographically and temporally weighted regression model. Remote Sens. Environ. *198*, 140–149.

He, Q., and Huang, B. (2018). Satellite-based mapping of daily high-resolution ground PM2.5 in China via space-time regression modeling. Remote Sens. Environ. *206*, 72–83.

Holstius, D.M., Pillarisetti, A., Smith, K.R., and Seto, E. (2014). Field calibrations of a low-cost aerosol sensor at a regulatory monitoring site in California. Atmospheric Meas. Tech. *7*, 1121–1131.

Holzworth, G. (1964). Extimates of mean maximum mixing depths in the contiguous United States. Mon. Weather Rev. *92*, 235–242.

Holzworth, G.C. (1967). Mixing Depths, Wind Speeds and Air Pollution Potential for Selected Locations in the United States. J. Appl. Meteorol. *6*, 1039–1044.

Jin, X., Fiore, A.M., Curci, G., Lyapustin, A., Civerolo, K., Ku, M., Donkelaar, A. van, and Martin, R.V. (2019). Assessing uncertainties of a geophysical approach to estimate surface fine particulate matter distributions from satellite-observed aerosol optical depth. Atmospheric Chem. Phys. *19*, 295–313.

Johnson, R.H., Ciesielski, P.E., and Cotturone, J.A. (2001). Multiscale Variability of the Atmospheric Mixed Layer over the Western Pacific Warm Pool. J. Atmospheric Sci. *58*, 2729–2750.

Karimian, H., Li, Q., Li, C., Jin, L., Fan, J., and Li, Y. (2016). An improved method for monitoring fine particulate matter mass concentrations via satellite remote sensing. Aerosol Air Qual. Res. *16*, 1081–1092.

Koschmieder, H. (1925). Theorie der horizontalen sichtweite II: Kontrast und sichtweite. Beitr. Zur Phys. Freien Atmosphäre 171−181.

Kumar, P., Morawska, L., Martani, C., Biskos, G., Neophytou, M., Di Sabatino, S., Bell, M., Norford, L., and Britter, R. (2015). The rise of low-cost sensing for managing air pollution in cities. Environ. Int. *75*, 199–205.

Levy, R.C., Mattoo, S., Munchak, L.A., Remer, L.A., Sayer, A.M., Patadia, F., and Hsu, N.C. (2013). The Collection 6 MODIS aerosol products over land and ocean. Atmos Meas Tech *6*, 2989–3034.

Lin, C., Li, Y., Yuan, Z., Lau, A.K.H., Li, C., and Fung, J.C.H. (2015). Using satellite remote sensing data to estimate the high-resolution distribution of ground-level PM2.5. Remote Sens. Environ. *156*, 117–128.

Lin, C., Lau, A.K.H., Fung, J.C.H., Lao, X.Q., Li, Y., and Li, C. (2019). Assessing the Effect of the Long-Term Variations in Aerosol Characteristics on Satellite Remote Sensing of PM2.5 Using an Observation-Based Model. Environ. Sci. Technol. *53*, 2990–3000.

Lin, C.Q., Li, Y., Lau, A.K.H., Deng, X.J., Tse, K.T., Fung, J.C.H., Li, C.C., Li, Z.Y., Lu, X.C., Zhang, X.G., et al. (2016). Estimation of long-term population exposure to PM2.5 for dense urban areas using 1-km MODIS data. Remote Sens. Environ. *179*, 13–22.

Lin, C.Q., Liu, G., Lau, A.K.H., Li, Y., Li, C.C., Fung, J.C.H., and Lao, X.Q. (2018). High-resolution satellite remote sensing of provincial PM2.5 trends in China from 2001 to 2015. Atmos. Environ. *180*, 110–116.

Liu, Y. (2014). Monitoring PM2.5 from Space for Health: Past, Present, and Future Directions. Env. Manage 6–10.

Ma, Z., Hu, X., Sayer, A.M., Levy, R., Zhang, Q., Xue, Y., Tong, S., Bi, J., Huang, L., and Liu, Y. (2016). Satellite-Based Spatiotemporal Trends in PM2.5 Concentrations: China, 2004–2013. Environ. Health Perspect. *124*, 184–192.

Mikhailuta, S.V., Taseiko, O.V., Pitt, A., Lezhenin, A.A., and Zakharov, Y.V. (2009). Seasonal variations of air pollutant concentrations within Krasnoyarsk City. Environ. Monit. Assess. *149*, 329–341.

Ministry of Environmental Management (2018). Governmental Report about the conditions and Protection of Environment. Offeset Ltd Kemerovo Russ.

Morawska, L., Thai, P.K., Liu, X., Asumadu-Sakyi, A., Ayoko, G., Bartonova, A., Bedini, A., Chai, F., Christensen, B., Dunbabin, M., et al. (2018). Applications of low-cost sensing technologies for air quality monitoring and exposure assessment: How far have they gone? Environ. Int. *116*, 286–299.

Ng, J. (2016). Comparison of PM2.5 Measurements Using the AirVisual Monitor and Beta Attenuation Monitor. accessed 29 August, 2019.

Peng, J., Chen, S., Lü, H., Liu, Y., and Wu, J. (2016). Spatiotemporal patterns of remotely sensed PM2.5 concentration in China from 1999 to 2011. Remote Sens. Environ. *174*, 109–121.

Pinder, R.W., Klopp, J.M., Kleiman, G., Hagler, G.S.W., Awe, Y., and Terry, S. (2019). Opportunities and challenges for filling the air quality data gap in low- and middle-income countries. Atmos. Environ. *215*, 116794.

Popoola, O.A.M., Carruthers, D., Lad, C., Bright, V.B., Mead, M.I., Stettler, M.E.J., Saffell, J.R., and Jones, R.L. (2018). Use of networks of low cost air quality sensors to quantify air quality in urban settings. Atmos. Environ. *194*, 58–70.

Rohde, R.A., and Muller, R.A. (2015). Air Pollution in China: Mapping of Concentrations and Sources. PLOS ONE *10*, e0135749.

Rolph, G., Stein, A., and Stunder, B. (2017). Environmental Modelling & Software Real-time Environmental Applications and Display sYstem : READY. Environ. Model. Softw. *95*, 210–228.

Schneider, P., Castell, N., Vogt, M., Dauge, F.R., Lahoz, W.A., and Bartonova, A. (2017). Mapping urban air quality in near real-time using observations from low-cost sensors and model information. Environ. Int. *106*, 234–247.

Seibert, P., Beyrich, F., Gryning, S.-E., Joffre, S., Rasmussen, A., and Tercier, P. (2000). Review and intercomparison of operational methods for the determination of the mixing height. Atmos. Environ. *34*, 1001–1027.

Semple, S., Ibrahim, A.E., Apsley, A., Steiner, M., and Turner, S. (2015). Using a new, low-cost air quality sensor to quantify second-hand smoke (SHS) levels in homes. Tob. Control *24*, 153–158.

Shaddick, G., Thomas, M.L., Green, A., Brauer, M., Donkelaar, A. van, Burnett, R., Chang, H.H., Cohen, A., Dingenen, R.V., Dora, C., et al. (2018). Data integration model for air quality: a hierarchical approach to the global estimation of exposures to ambient air pollution. J. R. Stat. Soc. Ser. C Appl. Stat. *67*, 231–253.

Singer, B.C., and Delp, W.W. (2018). Response of consumer and research grade indoor air quality monitors to residential sources of fine particles. Indoor Air *28*, 624–639.

Smolyakov, B.S., Makarov, V.I., Shinkorenko, M.P., Popova, S.A., and Bizin, M.A. (2014). Effects of Siberian wildfires on the chemical composition and acidity of atmospheric aerosols of remote urban, rural and background territories. Environ. Pollut. *188*, 8–16.

Snyder, E.G., Watkins, T.H., Solomon, P.A., Thoma, E.D., Williams, R.W., Hagler, G.S.W., Shelow, D., Hindin, D.A., Kilaru, V.J., and Preuss, P.W. (2013). The Changing Paradigm of Air Pollution Monitoring. Environ. Sci. Technol. *47*, 11369–11377.

Strukova E., Golub A., Markandya A. (2019). Air pollution costs in Ukraine. Environmental Economics, 2 (3), 52-63.

Su, T., Li, J., Li, C., Xiang, P., Lau, A.K.-H., Guo, J., Yang, D., and Miao, Y. (2017). An intercomparison of long-term planetary boundary layer heights retrieved from CALIPSO, ground-based lidar, and radiosonde measurements over Hong Kong. J. Geophys. Res. Atmospheres *122*, 3929–3943.

Tan, B.K. (2017). Laboratory Evaluation of Low to Medium Cost Particle Sensors. UWSpace *http://hdl.handle.net/10012/12776*.

U.S. EPA (2014). Fiscal Year 2014-2018 EPA Strategic Plan (Washington D.C., USA).

Watson, J.G. (2002). Visibility: Science and Regulation. J. Air Waste Manag. Assoc. *52*, 628–713.

WMO (2018). Low-cost sensors for the measurement of atmospheric composition: overview of topic and future applications. https://www.wmo.int/pages/prog/arep/gaw/documents/Low_cost_sensors_18_Oct.pdf.

Xiao, Q., Chang, H.H., Geng, G., and Liu, Y. (2018). An Ensemble Machine-Learning Model To Predict Historical PM2.5 Concentrations in China from Satellite Data. Environ. Sci. Technol. *52*, 13260–13269.

Yang, D., Li, C., Lau, A.K.-H., and Li, Y. (2013). Long-term measurement of daytime atmospheric mixing layer height over Hong Kong. J. Geophys. Res. Atmospheres *118*, 2422–2433.